

# Damped driven coupled oscillators: entanglement, decoherence and the classical limit

R D Guerrero Mancilla, R R Rey-González and K M Fonseca-Romero

Grupo de Óptica e Información Cuántica, Departamento de Física,  
Universidad Nacional de Colombia, Bogotá, Colombia

E-mail: [rdguerrerom@unal.edu.co](mailto:rdguerrerom@unal.edu.co), [rrreyg@unal.edu.co](mailto:rrreyg@unal.edu.co) and [kmfonsecar@unal.edu.co](mailto:kmfonsecar@unal.edu.co)

Received 24 September 2008, in final form 8 January 2009

Published 17 February 2009

Online at [stacks.iop.org/JPhysA/42/105302](http://stacks.iop.org/JPhysA/42/105302)

## Abstract

We investigate the quantum-classical border, the entanglement and decoherence of an analytically solvable model, comprising a first subsystem (a harmonic oscillator) coupled to a driven and damped second subsystem (another harmonic oscillator). We choose initial states whose dynamics is confined to a couple of two-level systems, and show that the maximum value of entanglement between the two subsystems, as measured by concurrence, depends on the dissipation rate to the coupling-constant ratio and the initial state. While in a related model the entropy of the first subsystem (a two-level system) never grows appreciably (for large dissipation rates), in our model it reaches a maximum before decreasing. Although both models predict small values of entanglement and dissipation, for fixed times of the order of the inverse of the coupling constant and large dissipation rates, these quantities decrease faster, as a function of the ratio of the dissipation rate to the coupling constant, in our model.

PACS numbers: 03.65.Ud, 03.67.Mn, 42.50.Pq, 89.70.Cf

## 1. Introduction

One expects quantum theory to approach to the classical theory, for example in the singular limit of a vanishing Planck's constant,  $\hbar \rightarrow 0$ , or for large quantum numbers. However, dissipative systems can bring forth some surprises: for example, QED (quantum electrodynamics) cavity fields interacting with two-level systems, may exhibit classical or quantum behavior, even if the system is kept at very low temperatures and if the mean number of photons in the cavity is of the order of one [1, 2], depending on the strength of the damping constant. Classical behavior, in this context refers to the unitary evolution of one of the subsystems, as if the other subsystem could be replaced by a classical driving. In QED cavities, the atom, which enters in one of the relevant Rydberg states (almost in resonance with the field sustained in

the cavity), conserves its purity and suffers a unitary rotation inside the cavity—exactly as if it were controlled by a classical driving field—without entangling with the electromagnetic field. This unexpected behavior was analyzed in [1] employing several short-time approximations, and it was found that in the time needed to rotate the atom, its state remains almost pure.

Other driven damped systems, composed by two (or more) subsystems can readily be identified. Indeed, in recent years there has been a rapid development of quite different physical systems and interfaces between them, including electrodynamic cavities [3], superconducting circuits [4, 5], confined electrons [6–8] and nanoresonators [9–11] on which it is possible to explore genuine quantum effects at the level of a few excitations and/or in individual systems. For instance, the interaction atom-electromagnetic field is exploited in experiments with trapped ions [12, 13], cavity electrodynamics and ensembles of atoms interacting with coherent states of light [14], radiation pressure over reflective materials in experiments coupling the mechanical motion of nanoresonators to light [11] and the coupling of cavities with different quality factors in the manufacturing of more reliable Ramsey zones [15]. In many of these interfaces it is possible to identify a system which couples strongly to the environment and another which couples weakly. For example, in the experiments of Haroche the electromagnetic field decays significantly faster [17] (or significantly slower [15]) than the atoms, the quality factor  $Q$  of the nanoresonators is much smaller than that of the cavity and the newest Ramsey zones comprise two coupled cavities of quite different  $Q$ . Several of these systems, therefore, can be modeled as coupled harmonic oscillators, one which can be considered dissipationless.

In this contribution we study an exactly solvable system, composed of two oscillators, which permits the analysis of large times, shedding additional light on the classical-quantum border. Entanglement and entropy, as measured by concurrence and linear entropy, are used to tell ‘classical’ from quantum effects.

## 2. The model

The system that we consider in this paper comprises two oscillators of natural frequencies  $\omega_1$  and  $\omega_2$ , coupled through an interaction which conserves the (total) number of excitations and whose coupling constant abruptly changes from zero to  $g$  at some initial time and back to zero at some final time. We take into account that the second oscillator loses excitations at the rate  $\gamma$ , through a phenomenological Liouvillian of Lindblad form, corresponding to zero temperature, in the dynamical equation of motion [18]. Lindblad superoperators are convenient because they preserve important characteristics of physically realizable states, namely hermiticity, conservation of the trace and semi-positivity [19]. In order to guarantee the presence of excitations, the second oscillator is driven by a classical resonant field.

There are several physical systems within reach of the currently available technology realizing the model just described. Coupled microcavities (for example structures consisting of a top distributed Bragg reflector (DBR) mirror, one GaAs vertical cavity, a coupling common DBR mirror, another GaAs cavity and a bottom DBR mirror) have been grown by molecular beam epitaxy [20]. Varying the number of AlAs/ $\text{Al}_x\text{Ga}_{1-x}\text{As}$  quarter-wavelength layers of the mirrors, it is possible to produce a bottom cavity with a photon lifetime much larger than that of the top cavity. If we drive the top cavity with classical light from the outside, the experimental setup is completed. In other possible scenario optical-fiber Fabry–Pérot cavities [21] can be coupled by a connecting fiber. The dissipation properties of the cavities depend on the alignment of the faces of the fiber tips defining them and the losses in the fibers. The proposal of coupled QED cavities [22, 23] constitutes a third possible physical realization of the model considered here. We finally want to draw attention to a system in use in recent QED

experiments [16]: a  $Q = 2 \times 10^3$  cavity weakly coupled to a cavity with  $Q < 200$ , which realizes the model analyzed here.

The interaction can be considered to be turned on (off) in the remote past (remote future) if it is always present (coupled Ramsey zones or coupled microcavities), or can be present for a finite time interval. The initial states of the coupled oscillators also depend on the experimental setup, varying from the base state of the compound system to a product of the steady state of the coupled damped oscillator with the state of the other oscillator.

All the ingredients detailed before can be summararily put into the Liouville–von Neumann equation for the density matrix  $\hat{\rho}$  of the total system,

$$\frac{d\hat{\rho}}{dt} = -\frac{i}{\hbar}[\hat{H}, \hat{\rho}] + \gamma(2\hat{a}\hat{\rho}\hat{a}^\dagger - \hat{a}^\dagger\hat{a}\hat{\rho} - \hat{\rho}\hat{a}^\dagger\hat{a}), \quad (1)$$

where  $\hat{H}$  is the total Hamiltonian of the system and the second term of the rhs of (1) is the Lindblad superoperator which accounts for the loss of excitations of the second oscillator. In absence of the coupling with the first oscillator, the inverse of twice the dissipation rate  $\gamma$  gives the mean lifetime of the second oscillator. The first two terms of the total Hamiltonian,

$$\hat{H} = \hbar\omega_1\hat{b}^\dagger\hat{b} + \hbar\omega_2\hat{a}^\dagger\hat{a} + \hbar g(\Theta(t) - \Theta(t+T))(\hat{a}^\dagger\hat{b} + \hat{a}\hat{b}^\dagger) + i\hbar\epsilon(e^{-i\omega_D t}\hat{a}^\dagger - e^{i\omega_D t}\hat{a}) \quad (2)$$

are the free Hamiltonians of the two harmonic oscillators; the next term, which is modulated by the step function  $\Theta(t)$  is the interaction between them and the last term is the driving. The bosonic operators of creation  $\hat{b}$  ( $\hat{a}$ ) and annihilation  $\hat{b}^\dagger$  ( $\hat{a}^\dagger$ ) of one excitation of the first (second) oscillator satisfy the usual commutation relations. From here on we focus on the case of resonance,  $\omega_1 = \omega_2 = \omega_D = \omega$ . The interaction time  $T$  is left indefinite until the end of the paper, where we compare our results with those of a related model.

### 3. Dynamical evolution

The solution of the dynamical equation (1) can be written as

$$\hat{\rho}(t) = \mathcal{D}(\beta(t), \alpha(t))\tilde{\rho}(t)\mathcal{D}^\dagger(\beta(t), \alpha(t)), \quad (3)$$

where  $\mathcal{D}(\beta(t), \alpha(t))$  is the two-mode displacement operator,

$$\mathcal{D}(\beta(t), \alpha(t)) = \mathcal{D}_1(\beta(t))\mathcal{D}_2(\alpha(t)) = e^{\beta(t)\hat{b}^\dagger - \beta^*(t)\hat{b}} e^{\alpha(t)\hat{a}^\dagger - \alpha^*(t)\hat{a}},$$

and  $\tilde{\rho}(t)$  is the total density operator in the interaction picture defined by equation (3). By replacing (3) into (1), and employing the operator identities

$$\frac{d}{dt}\mathcal{D}(\alpha) = \left(-\frac{\alpha^*\dot{\alpha} - \dot{\alpha}^*\alpha}{2} + \dot{\alpha}\hat{a}^\dagger - \dot{\alpha}^*\hat{a}\right)\mathcal{D}(\alpha) = \mathcal{D}(\alpha) \left(\frac{\alpha^*\dot{\alpha} - \dot{\alpha}^*\alpha}{2} + \dot{\alpha}\hat{a}^\dagger - \dot{\alpha}^*\hat{a}\right),$$

with the dot designating the time derivative as usual, we are able to decouple the dynamics of the displacement operators, obtaining the following dynamical equations for the labels  $\alpha$  and  $\beta$ ,

$$\frac{d}{dt} \begin{pmatrix} \alpha \\ \beta \end{pmatrix} = \begin{pmatrix} -\gamma - i\omega & -ig \\ -ig & -i\omega \end{pmatrix} \begin{pmatrix} \alpha \\ \beta \end{pmatrix} + \begin{pmatrix} \epsilon e^{-i\omega t} \\ 0 \end{pmatrix}, \quad (4)$$

for times between zero and  $T$ . On the other hand, the ansatz (3) also provides the equation of motion for  $\tilde{\rho}(t)$ , which turns out to be very similar to (1) but with the Hamiltonian  $\tilde{H} = \hat{H}(\epsilon = 0)$ , that is, without driving. The separation provided by our ansatz is also appealing from the point of view of its possible physical interpretation, because the effect of the driving has been singled out and quantum (entangling and purity) effects are extracted from the displaced density operator  $\tilde{\rho}(t)$ .

We assume that the two oscillators interact only after the second oscillator reaches its stationary coherent state,

$$\hat{\rho}_2(t) = \text{tr}_1 \hat{\rho}(t) = \left| \frac{\epsilon}{\gamma} e^{-i\omega t} \right\rangle \left\langle \frac{\epsilon}{\gamma} e^{-i\omega t} \right|, \quad (5)$$

which is obtained by solving (4) with the interaction turned off. If we want a mean number of excitations of the order of one then the driving amplitude must satisfy  $\epsilon \approx \gamma$  and thereby the larger the dissipation is, the larger the driving is to be chosen. We suppose that at zero time, when the oscillators begin to interact, the state of the total system is separable with the second oscillator state given by (5). It is technically convenient to consider the state of the first oscillator as a linear combination of its ground and first excited states because we will be able to quantify the entanglement between the oscillators. Thus, the initial state  $\hat{\rho}(0)$  given by

$$\mathcal{D} \left( 0, \frac{\epsilon}{\gamma} \right) \underbrace{(\cos(\theta)|0\rangle + \sin(\theta)|1\rangle)(\cos(\theta)\langle 0| + \sin(\theta)\langle 1|) \otimes |0\rangle\langle 0|}_{\hat{\rho}(0)} \mathcal{D}^\dagger \left( 0, \frac{\epsilon}{\gamma} \right), \quad (6)$$

corresponds to a state of the form described by equation (3) with  $\beta(0) = 0$  and  $\alpha(0) = \epsilon/\gamma$ . At later times, the solution maintains the same structure, but—as can be seen from the solution of (4)—the labels of the displacement operators evolve as follows:

$$\alpha(t) = \epsilon e^{-\frac{1}{2}(\gamma+2i\omega)t} \left\{ \frac{1}{\gamma} \cos(\tilde{g}t) + \frac{\sin(\tilde{g}t)}{2\tilde{g}} \right\}, \quad (7)$$

$$\beta(t) = -\frac{i e^{-i\omega t} \epsilon}{g} + \frac{i\epsilon}{g} e^{-\frac{1}{2}(\gamma+2i\omega)t} \left\{ \cos(\tilde{g}t) + (-2g^2 + \gamma^2) \frac{\sin(\tilde{g}t)}{2\gamma\tilde{g}} \right\}, \quad (8)$$

where we have defined the new constant  $\tilde{g} = \frac{1}{2}\sqrt{4g^2 - \gamma^2}$ . We employ  $\tilde{g}$ , which also appears in the solution of the displaced density operator, to define three different regimes: underdamped ( $\tilde{g}^2 > 0$ ), critically damped ( $\tilde{g}^2 = 0$ ) and overdamped ( $\tilde{g}^2 < 0$ ) regime. It is important to note that there is no direct connection with the quality factor of the damped oscillator: it is possible to have physical systems in the overdamped regime defined here even with relatively large quality factors if the interaction constant  $g$  is much smaller than  $\omega$ , the frequency of the oscillators.

The inspection of the equations (7) and (8), allows one to clearly identify the time scale  $2/\gamma$ , after which the stationary state is reached and the state of the first oscillator just rotates with frequency  $\omega$  and has a mean number of excitations equal to  $\epsilon^2/g^2$ . The doubling of the damping time of the second oscillator, from  $1/\gamma$  in the absence of interaction to  $2/\gamma$ , in the underdamped regime, can be seen as an instance of the shelving effect [24]. The first oscillator, which in absence of interaction, suffers no damping, it is now driven and damped. It can be thought that the excitations remain half of the time on each oscillator, and that they decay (when they are in the second oscillator) with a damping constant  $\gamma$ , thereby leading to an effective damping constant of  $\gamma/2$ . An interesting feature of the solution is that the displacement of the second oscillator goes to zero, for times much larger than  $1/\gamma$ . In the stationary state, the first oscillator evolves as if it were driven by a classical field  $-i\hbar\epsilon \exp(-i\omega t)$  and damped with a damping rate  $g$ , without any interaction with a second oscillator. More generally speaking, we remark that from the point of view of the first oscillator, the evolution of its displacement operator happens as if there were damping but no coupling, and the driving were of the form  $\hbar g(\beta - i\alpha)$ , or, in terms of the parameters of the problem,

$$F(t) = -i\hbar\epsilon e^{-i\omega t} - i\hbar\epsilon e^{-(\gamma/2+i\omega)t} \left( \left( \frac{g}{\gamma} - 1 \right) \cos(\tilde{g}t) + \frac{2g^2 + g\gamma - \gamma^2}{2\gamma\tilde{g}} \sin(\tilde{g}t) \right). \quad (9)$$

This behavior is particularly relevant in the following extreme case, whose complete solution depends only on the displacement operators. If the initial state of the first oscillator is the ground state then  $\tilde{\rho}$  does not evolve in time, i.e. it remains in the state  $|00\rangle$ , and the total pure and separable joint state is

$$\rho(t) = |\beta(t)\rangle\langle\beta(t)| \otimes |\alpha(t)\rangle\langle\alpha(t)|. \quad (10)$$

Even in the more general case considered here, corresponding to the initial state (6), the solution of  $\tilde{\rho}(t)$  possesses only a few non-zero elements. If we write the total density operator as

$$\tilde{\rho}(t) = \sum_{i_1 i_2 j_1 j_2} \tilde{\rho}_{i_1 i_2}^{j_1 j_2} |i_1 i_2\rangle\langle j_1 j_2|, \quad (11)$$

we can arrange the elements corresponding to zero and one excitations in each oscillator, as the two-qubit density matrix

$$\begin{pmatrix} \tilde{\rho}_{00}^{00}(t) & \tilde{\rho}_{00}^{01}(t) & \tilde{\rho}_{00}^{10}(t) & 0 \\ \tilde{\rho}_{01}^{00}(t) & \tilde{\rho}_{01}^{01}(t) & \tilde{\rho}_{01}^{10}(t) & 0 \\ \tilde{\rho}_{10}^{00}(t) & \tilde{\rho}_{10}^{01}(t) & \tilde{\rho}_{10}^{10}(t) & 0 \\ 0 & 0 & 0 & 0 \end{pmatrix}. \quad (12)$$

If we measure time in units of  $g$  by defining  $t' = gt$  we have only two free parameters  $\Gamma = \gamma/g$  and  $\Omega = \omega/g$ . The non-vanishing elements of the density matrix, written in the underdamped case ( $|\Gamma| < 2$ ), are given by (hermiticity of the density operator yields the missing non-zero elements)

$$\begin{aligned} \tilde{\rho}_{00}^{00}(t') &= 1 - \sin^2 \theta e^{-\Gamma t'} \left( \frac{4 - \Gamma^2 \cos(\sqrt{4 - \Gamma^2} t')}{4 - \Gamma^2} - \frac{\Gamma \sin(\sqrt{4 - \Gamma^2} t')}{\sqrt{4 - \Gamma^2}} \right), \\ \tilde{\rho}_{01}^{01}(t') &= 2 \sin^2(\theta) e^{-\Gamma t'} \frac{1 - \cos(\sqrt{4 - \Gamma^2} t')}{4 - \Gamma^2}, \\ \tilde{\rho}_{10}^{10}(t') &= \sin^2(\theta) e^{-\Gamma t'} \left( \frac{(2 - \Gamma^2) \cos(\sqrt{4 - \Gamma^2} t') + 2}{4 - \Gamma^2} - \frac{\Gamma \sin(\sqrt{4 - \Gamma^2} t')}{\sqrt{4 - \Gamma^2}} \right), \\ \tilde{\rho}_{01}^{00}(t') &= i \sin(2\theta) e^{i\Omega t' - \frac{\Gamma t'}{2}} \frac{\sin(\sqrt{4 - \Gamma^2} \frac{t'}{2})}{\sqrt{4 - \Gamma^2}}, \\ \tilde{\rho}_{10}^{00}(t') &= \frac{\sin(2\theta)}{2} e^{i\Omega t' - \frac{\Gamma t'}{2}} \left( \cos\left(\sqrt{4 - \Gamma^2} \frac{t'}{2}\right) - \frac{\Gamma \sin(\sqrt{4 - \Gamma^2} \frac{t'}{2})}{\sqrt{4 - \Gamma^2}} \right), \\ \tilde{\rho}_{10}^{01}(t') &= 2i \sin^2(\theta) e^{-\Gamma t'} \frac{\sin(\sqrt{4 - \Gamma^2} \frac{t'}{2})}{\sqrt{4 - \Gamma^2}} \left( \frac{\Gamma \sin(\sqrt{4 - \Gamma^2} \frac{t'}{2})}{\sqrt{4 - \Gamma^2}} - \cos\left(\sqrt{4 - \Gamma^2} \frac{t'}{2}\right) \right). \end{aligned}$$

The expressions of the elements of the density matrix in the critically damped case  $\Gamma = 2$  and in the overdamped case  $\Gamma > 2$  can be obtained from those given in the text for the underdamped case  $\Gamma < 2$ .

#### 4. Entanglement

Although quantities such as quantum discord [25] have been proposed to extract the quantum content of correlations between two systems, we presently quantify the quantum correlations between both oscillators employing a measure of entanglement. Due to the dynamics of

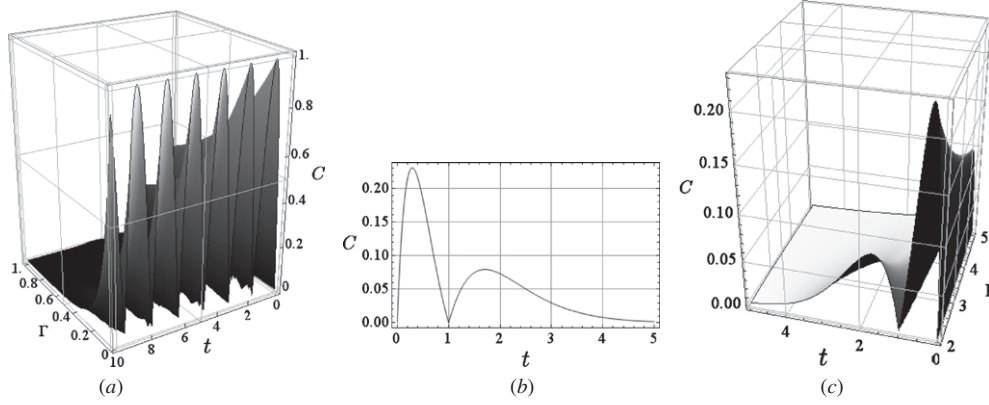


**Figure 1.** Concurrence as a function of time and the rescaled damping constant in the (a) underdamped, (b) critically damped and (c) overdamped case.

the system, and the initial states chosen, the whole system behaves as a couple of qubits and therefore its entanglement can be measured by Wootters' concurrence [26]. One of the most important characteristics of the form of the solution given by (3) is that concurrence, as well as linear entropy, depends *only* on the displaced density operator  $\tilde{\rho}(t')$ . In our case the concurrence reduces to

$$\begin{aligned}
 C(t') &= \left| \sqrt{\tilde{\rho}_{10}^{01}(t')\tilde{\rho}_{01}^{10}(t')} + \sqrt{\tilde{\rho}_{01}^{01}(t')\tilde{\rho}_{10}^{10}(t')} \right| - \left| \sqrt{\tilde{\rho}_{10}^{01}(t')\tilde{\rho}_{01}^{10}(t')} - \sqrt{\tilde{\rho}_{01}^{01}(t')\tilde{\rho}_{10}^{10}(t')} \right| \\
 &= 2\sqrt{\tilde{\rho}_{10}^{01}(t')\tilde{\rho}_{01}^{10}(t')} = 2|\tilde{\rho}_{01}^{10}(t')|,
 \end{aligned}
 \tag{13}$$

where the positivity and hermiticity of the density matrix were used. The explicit expressions for the concurrence in the underdamped (UD), critically damped (CD) and overdamped (OD) regimes are

$$\begin{aligned}
 C_{UD}(t') &= 4 \sin^2(\theta) e^{-\Gamma t'} \frac{\sin\left(\frac{\sqrt{4-\Gamma^2}t'}{2}\right)}{\sqrt{4-\Gamma^2}} \left| \frac{\Gamma \sin\left(\frac{\sqrt{4-\Gamma^2}t'}{2}\right)}{\sqrt{4-\Gamma^2}} - \cos\left(\frac{\sqrt{4-\Gamma^2}t'}{2}\right) \right|, \\
 C_{CD}(t') &= 2 \sin^2(\theta) e^{-2t'} t' |t' - 1|, \\
 C_{OD}(t') &= 4 \sin^2(\theta) e^{-\Gamma t'} \frac{\sinh\left(\frac{\sqrt{\Gamma^2-4}t'}{2}\right)}{\sqrt{\Gamma^2-4}} \left| \frac{\Gamma \sinh\left(\frac{\sqrt{\Gamma^2-4}t'}{2}\right)}{\sqrt{\Gamma^2-4}} - \cosh\left(\frac{\sqrt{\Gamma^2-4}t'}{2}\right) \right|.
 \end{aligned}
 \tag{14}$$

All the dependence on the initial state is contained in the squared norm of the coefficient of the state  $|1\rangle$  of the displaced density operator. In all regimes the concurrence vanishes at zero time because the initial state considered is separable. However, while in the underdamped case the concurrence vanishes periodically (see equation (15)), in the other two cases it crosses zero once ( $t > 0$ ) and reaches zero asymptotically as time grows. This shows a markedly different qualitative behavior (see figures 1 and 2).

In the underdamped regime the zeroes of the concurrence are found at times

$$\tau_{1n} = \frac{2n\pi}{\sqrt{4-\Gamma^2}}, \quad \text{and} \quad \tau_{2n} = \frac{2\pi n + 2 \arccos\left(\frac{\Gamma}{2}\right)}{\sqrt{4-\Gamma^2}},
 \tag{15}$$

where  $n$  is a non-negative integer. In this contribution, the inverse sine and inverse cosine functions are chosen to take values in the interval  $[0, \pi/2]$ . The time  $\tau_{10}$  corresponds to the initial state. The sequence of concurrence zeroes is thereby  $0 = \tau_{10} < \tau_{20} < \tau_{11} < \tau_{21} \dots$ . As

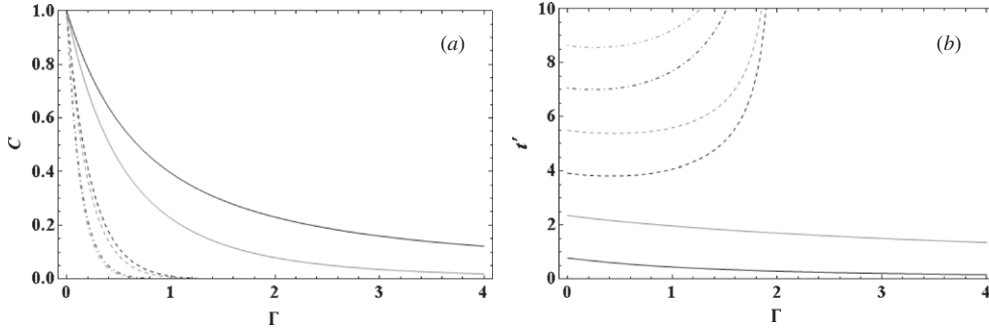


**Figure 2.** (a) Concurrence local maxima at times  $\tau_{+(-)n}$  in black (gray) color for  $n = 0$  full line,  $n = 1$  dashed line and  $n = 2$  dashed-dot line and (b) times of maximum values of concurrence, as a function of the rescaled damping constant.

the critical damping is approached, the time  $\tau_{11}$  is pushed toward infinity, while  $\tau_{20}$  approaches the finite time  $2/\Gamma$  (see figure 2). For the initial states considered in this paper we do not observe the sudden death of the entanglement since the concurrence is zero only for isolated instants of time.

If one writes the concurrence in the underdamped regime in the alternative form,

$$C_{UD}(t') = \frac{\sin^2 \theta}{2(1 - \Gamma^2/4)} e^{-\Gamma t'} \left| \frac{\Gamma}{2} - \sin \left( \arcsin \left( \frac{\Gamma}{2} \right) + 2\sqrt{1 - \frac{\Gamma^2}{4}} t' \right) \right|, \quad (16)$$

it is easy to verify that at the times  $\tau_{\pm n}$ , given by

$$\tau_{\pm n} = \frac{1}{\sqrt{4 - \Gamma^2}} \left( (2n + 1)\pi \pm \arccos \left( \frac{\Gamma^2}{4} \right) - 2 \arcsin \left( \frac{\Gamma}{2} \right) \right) > 0, \quad n = 0, 1, \dots, \quad (17)$$

the concurrence reaches the local maxima

$$C_{\pm n} = \sin^2 \theta \left( \sqrt{1 + \frac{\Gamma^2}{4}} \pm \frac{\Gamma}{2} \right) \exp \left( - \frac{\Gamma \left( (2n + 1)\pi \pm \arccos \left( \frac{\Gamma^2}{4} \right) - 2 \arcsin \left( \frac{\Gamma}{2} \right) \right)}{2\sqrt{1 - \frac{\Gamma^2}{4}}} \right).$$

We observe these maxima to lie on the curves  $\sin^2 \theta K_{\pm} \exp(-\Gamma t)$ , where the constants  $K_{\pm} = \sqrt{1 + \frac{\Gamma^2}{4}} \pm \frac{\Gamma}{2}$  satisfy the inequalities  $\sqrt{2} - 1 \leq K_- \leq 1 \leq K_+ \leq \sqrt{2} + 1$ . Maxima of concurrence depend on both the initial state and the value of the rescaled damping constant, and reach the maximum available value of one only in the non-dissipative case for a particular initial state. In order to have negligible values of concurrence (except for small time intervals around the zeroes of concurrence) it is necessary to have times much larger than  $1/\gamma$ . From the point of view of classical-like behavior, the most favorable scenario corresponds to zero or almost zero concurrence, which are obtained for short time intervals around  $\tau_{1n}$ ,  $\tau_{2n}$  and for large values of time.

In the overdamped regime, the concurrence presents two maxima,  $\tau_-$  and  $\tau_+ > \tau_-$

$$\tau_{\pm} = \frac{2 \operatorname{arccosh}(\Gamma/2) \pm \operatorname{arccosh}(\Gamma^2/4)}{2\sqrt{1 - \Gamma^2/4}}, \quad (18)$$

both of which go to zero as the rescaled dissipation rate grows,  $\tau_+ \rightarrow 4 \ln(\Gamma)/\Gamma$  and  $\tau_- \rightarrow \ln(2)/\Gamma$  (see figure 2). The function  $\operatorname{arccosh}(x)$  is chosen to return non-negative

values for  $x \geq 1$ . Since the global maximum of concurrence, which corresponds to the later time, scales like  $1/(2\Gamma)$  for large values of  $\Gamma$ , in the highly overdamped regime quantum correlations are not developed at any time.

The behavior of concurrence in the different regimes is shown in figure 1. It is apparent that small values of concurrence are obtained for very small times and for large times in the underdamped case and for all times for a highly overdamped oscillator. In figure 2 we depict the times at which concurrence attains a maximum, and the maximum values of concurrence, as a function of the rescaled damping constant. One can see how the first two times of maximum concurrence go to zero, while the other times diverge, as the critically damped regime is reached. The first two maxima of concurrence vanish more slowly than the rest of maxima, which hit zero at  $\Gamma = 2$ .

## 5. Entropy

The entropy is analyzed employing the linear entropy of the first oscillator, the system of interest. As remarked before, the first oscillator behaves like a two-level system, where the maximum value of the linear entropy, 0.5, is obtained when the population of each of the two states is one half. The type of ‘classical’ behavior which allows the interaction with Ramsey zones to be modeled like a classical driving force occurs when the linear entropy is very small, and hence the state of the first oscillator is (almost) pure and uncorrelated with the state of the second oscillator. The linear entropy for the first oscillator can be computed as

$$\delta_1(t') = 1 - \text{tr}_1(\text{tr}_2 \rho \text{tr}_2 \rho) = 1 - \text{tr}_1(\text{tr}_2 \tilde{\rho} \text{tr}_2 \tilde{\rho}) = 2 \det(\text{tr}_2 \tilde{\rho}), \quad (19)$$

where the last equality holds for two-level systems. In equation (19) the density operator of the first oscillator is assumed to be represented by a  $2 \times 2$  matrix. Employing the expressions we have found for the elements of  $\tilde{\rho}$  we obtain

$$\delta_1(t') = 2 \sin^4 \theta x(t')(1 - x(t')), \quad (20)$$

where  $x$ , in the underdamped regime, is given by

$$x_{\text{UD}}(t) = \frac{e^{-\Gamma t} \sin^2(\sqrt{1 - \Gamma^2/4}t - \arccos(\Gamma/2))}{1 - \Gamma^2/4}. \quad (21)$$

Surprisingly, as in the case of concurrence, the influence of the initial state factors out in the expression of the linear entropy of the first oscillator, which turns out to be proportional to the square of the population of  $|1\rangle$  in the initial displaced operator. As it is well known, in the limit of zero dissipation, the linear entropy of the reduced density matrix is equal to one fourth of the square of the concurrence. At times  $\tau_{2n}$  (see equation (15)), when both concurrence and linear entropy vanish, the total state of the system is separable,  $\rho(g\tau_{2n}) = |\beta(g\tau_{2n})\rangle\langle\beta(g\tau_{2n})| \otimes \rho_2(g\tau_{2n})$ ; that is, from the point of view of the first oscillator the evolution is unitary like. Since the linear entropy begins at zero, because the initial state is pure and separable, there is a maximum in the interval  $(0, \tau_{20})$ , which turns out to give a linear entropy of exactly 0.5 (we treat the case  $\sin \theta = 1$ , because—due to the scaling property discussed before—a simple multiplication by  $\sin^4 \theta$  gives the result for other cases). Indeed, as the function  $x(t)$  changes continuously from  $x(t=0) = 1$  to  $x(t=\tau_{20}) = 0$ , it crosses 0.5 at some time  $\tau_{30}$  in between, giving the maximum value possible of the linear entropy. Although the exact value of  $\tau_{30}$  can be obtained only numerically, good analytical approximations can readily be obtained. For example,  $\tau_{30} \approx \pi/(4 + 4g + 2g^2)$ , gives an error smaller than 0.5%.

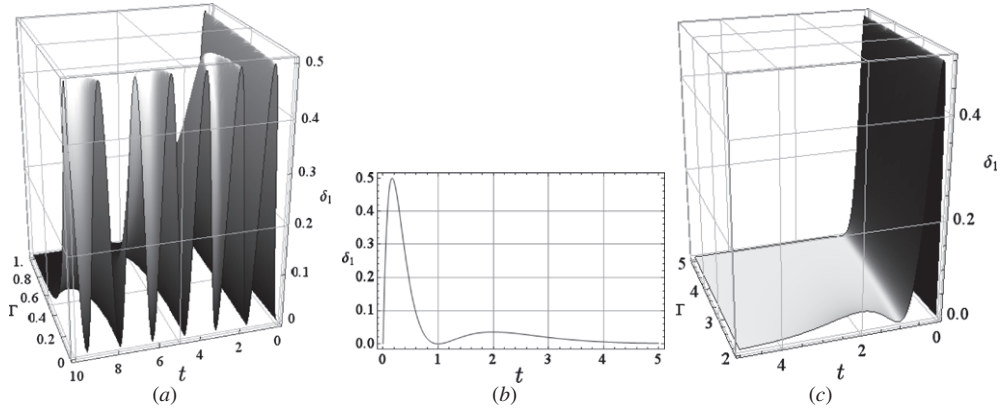


**Figure 3.** Linear entropy of the first oscillator as a function of time and the rescaled damping constant in the (a) underdamped, (b) critically damped and (c) overdamped case.

For small values of the rescaled damping constant,  $\Gamma \lesssim 0.237$ , there are several solutions to the equation  $x(t) = 0.5$  in the interval  $(0, \log(2)/\Gamma)$ , which give absolute maxima of the linear entropy, while the times

$$\tau_{4n} = \frac{2 \arccos(\Gamma/2) + n\pi}{\sqrt{1 - \Gamma^2/4}}, \quad n = 0, 1, 2, \dots, \quad (22)$$

correspond to local minima. In the interval  $(\log(2)/\Gamma, \infty)$  the times  $\tau_{4n}$  give local maxima. All of the local maxima and minima given by equation (22) belong to the curve  $2e^{-\Gamma t}(1 - e^{-\Gamma t})$ . The large time behavior of the local maxima of linear entropy and concurrence is, thereby, of the same form constant  $\times \exp(-\Gamma t)$ . For values of  $\Gamma > 0.237$  all times  $\tau_{4n}$  give local maxima. The maxima of concurrence and linear entropy coincide only in the weakly damped case, because concurrence and linear entropy are not independent for pure bipartite states.

At times  $\tau_{1n}$  (see equation (15)), where the total state  $\rho(g\tau_{1n}) = \rho_1(g\tau_{1n}) \otimes |\alpha(g\tau_{1n})\rangle\langle\alpha(g\tau_{1n})|$ , is separable, the reduced state of the first oscillator is mixed. The linear entropy is small for short ( $\tau_{1n} \ll \log(2)/\Gamma$ ) and large ( $\tau_{1n} \gg \log(2)/\Gamma$ ) times.

In the overdamped regime the function  $x(t)$ , which appears on the expression for linear entropy (20) and is given by

$$x_{OD}(t') = \frac{e^{-\Gamma t'} \sinh^2(\sqrt{\Gamma^2/4 - 1}t' - \text{arccosh}(\Gamma/2))}{\Gamma^2/4 - 1}, \quad (23)$$

begins at one for  $t' = 0$ , and goes down to zero for large values of time. The time at which it crosses one half can be calculated to be  $\tau_{0.5} \approx 0.16557 < 1/6$  for  $\Gamma = 2$  and for large values of  $\Gamma$  it goes as  $\tau_{0.5} \approx \ln 2/(2\Gamma)$ . It is easy to find interpolating functions with small error for the time of crossing,

$$\tilde{\rho}_{10}^{10} \left( t' = \frac{1}{6 + \frac{4}{\ln 2} \sinh(\text{arccosh}(\frac{\Gamma}{2}) \tanh(\frac{\text{arccosh}(\frac{\Gamma}{2})}{1.6}))} \right) = 0.5(1 + \Delta),$$

where  $|\Delta| < 2.5\%$ . It is interesting to note that for large values of the damping this time  $(\ln(2)/(2\Gamma))$  is half the time needed to obtain the maximum value of concurrence, and that, at the later time, the linear entropy is 3/4 of the maximum value of entropy, a relatively large value. The state of the first oscillator always becomes maximally mixed before becoming

pure again, no matter how large the value of the damping. We show the behavior of linear entropy in figure 3. In the underdamped regime there are infinite maxima and minima, while for critical damping and for the overdamped regime there are only two maxima. The first maximum always corresponds to a linear entropy of one half.

## 6. Conclusions

In the present contribution, we have shown that the classical quantum border in this model depends mainly on the initial state and on the damping constant to the interaction coupling ratio, and that quantum effects, characteristic of the underdamped regime, can be seen in the other regimes for small times. Here we want to compare our results with those of reference [1], where a model similar to ours is investigated. If we replace the first harmonic oscillator by a two-level system and employ a microscopic model for the bath, instead of the Lindblad operator, we obtain the model of a Ramsey zone studied in [1]. In order to make connection with Ramsey zones we set  $\omega \approx 10^{10}$  Hz,  $Q \approx 10^4$ ,  $g \approx 10^4$  Hz and  $T_R \approx 10^{-5}$  s, which was chosen to produce  $\pi/2$  pulse, that is a pulse that can rotate the state of the two-level system, as represented in a Bloch sphere, by an angle  $\pi/2$ . These numbers place the system into the highly overdamped (regime because  $\Gamma = \omega/(Qg) \approx 10^2 \gg 2$ ) and give a rescaled evolution time of the order of  $gT \approx 10^{-1}$ . Recent Ramsey zones employ smaller values of  $Q$  which push the system deeper into the highly overdamped regime. Here we use the values of  $\omega$ ,  $\gamma$  and  $g$  given above, and an evolution time of order  $1/g$ . Indeed, the Hamiltonian  $\hbar\omega\hat{b}^\dagger\hat{b} + \hbar g (\Theta(t) - \Theta(t+T)) (\alpha_0 e^{-i\omega t}\hat{b}^\dagger + \alpha_0^* e^{i\omega t}\hat{b})$ , with  $\|\alpha_0\| \approx 1$ —which would model the interaction of the first oscillator with a classical driving field of an average number of excitations of the order of one—has a characteristic time  $1/g$ , corresponding to  $T' \approx 1$ .

The dynamical behavior of the linear entropy obtained here, is quite different from that of [1]: there the linear entropy was never large for the relevant time interval, here it grows to the maximum possible for a two-level system, and then goes to zero very quickly. Therefore, in this model dissipation produces relaxation also, and a description obviating the second oscillator still needs a dissipation process. Although, at the evolution time  $T$ , both models predict a small atomic entropy, in Ramsey zones it decreases as  $\delta_1(T_R' \approx 0.1) \approx 4/\Gamma$ , while in the present model it goes to zero as  $\delta_1(T' \approx 1) \propto 1/\Gamma^4$ . Qualitative and quantitative differences notwithstanding, at the evolution time the linear entropy is very small, in both cases, due to the smallness of the ratio  $g/\gamma$ . As remarked before the quality factor of the damped oscillator does not appear directly in either case: it can be possible to have a very weakly damped oscillator and a highly overdamped interaction. However, as the first oscillator quality factor is improved, the damping constant will eventually be comparable with the interaction constant, and there will be considerable entanglement between both oscillators. For the same physical system if the damping rate can be changed then classical or quantum behavior can be obtained.

## Acknowledgments

This work was partially funded by DIB-UNAL and Facultad de Ciencias, Universidad Nacional (Colombia).

## References

- [1] Kim J I, Fonseca Romero K M, Horiguti A M, Davidovich L, Nemes M C and de Toledo Piza A F R 1999 Classical behavior with small quantum numbers: The physics of Ramsey interferometry of Rydberg atoms *Phys. Rev. Lett.* **82** 4737

- [2] Raimond J M, Brune M and Haroche S 2001 Colloquium: Manipulating quantum entanglement with atoms and photons in a cavity *Rev. Mod. Phys.* **73** 565
- [3] Mabuchi H and Doherty A C 2002 Decoherence, chaos and the second law *Rev. Mod. Phys.* **298** 1372
- [4] Majer J *et al* 2007 Coupling superconducting qubits via a cavity bus *Nature* **449** 443
- [5] Wallraff A, Schuster D, Blais A, Frunzio L, Huang R-S, Majer J, Kumar S, Girvin S M and Schoelkopf R J 2004 Circuit quantum electrodynamics: coherent coupling of a single photon to a Cooper pair box *Nature* **431** 162
- [6] Pioro-Ladriere M, Tokura Y, Obata T, Kubo T and Tarucha S 2007 Micro-magnets for coherent electron spin control in quantum dots *Appl. Phys. Lett.* **90** 024105
- [7] Engel H-A, Kouwenhoven L P, Loss D and Marcus C M 2004 Controlling spin qubits in quantum dots *Quantum Information Processing* **3** 115
- [8] Amasha S, MacLean K, Zumbühl D, Radu I, Kastner M A, Hanson M P and Gossard A C 2006 Toward the manipulation of a single spin in an AlGaAs/GaAs single-electron transistor *Proc. SPIE* **6244** 624419
- [9] Jacobs K 2007 Engineering quantum states of a nanoresonator via a simple auxiliary system *Phys. Rev. Lett.* **99** 117203
- [10] Vitali D *et al* 2007 Entangling a nanomechanical resonator and a superconducting microwave cavity *Phys. Rev. A* **76** 042336
- [11] Jayich A M, Sankey J C, Zwickl B M, Yang C, Thompson J D, Girvin S M, Clerk A A, Marquardt F and Harris J G E 2008 Dispersive optomechanics: a membrane inside a cavity *New J. Phys.* **10** 095008
- [12] Monroe C 2002 Quantum information processing with atoms and photons *Nature* **416** 238
- [13] Blinov B B, Moehring D L, Duan L M and Monroe C 2002 Observation of entanglement between a single trapped atom and a single photon *Nature* **428** 153
- [14] Sherson J F, Krauter H, Olsson R K, Julsgaard B, Hammerer K, Cirac I and Polzik E S 2006 Quantum teleportation between light and matter *Nature* **443** 557
- [15] Haroche S, Brune M and Raimond J M 2007 Measuring the photon number parity in a cavity: from light quantum jumps to the tomography of non-classical field states *Nature* **54** 2101
- [16] Gleyzes S, Kuhr S, Guerlin C, Bernu J, Deléglise S, Hoff U B, Brune M, Raimond J-M and Haroche S 2007 Quantum jumps of light recording the birth and death of a photon in a cavity *Nature* **446** 297
- [17] Brune M, Hagley E, Dreyer J, Maître X, Maali A, Wunderlich C, Haroche S and Raimond J M 1996 Observing the progressive decoherence of the meter in a quantum measurement *Phys. Rev. Lett.* **77** 4887
- [18] Louisell W H 1973 *Quantum Statistical Properties of Radiation* (New York: Wiley)
- [19] Lindblad G 1976 On the generators of quantum dynamical semigroups *Commun. Math. Phys.* **48** 119
- [20] Pellandini P, Stanley R P, Houdré R, Oesterle U and Ilegems M 1997 Dual-wavelength laser emission from a coupled semiconductor microcavity *App. Phys. Lett.* **71** 864
- [21] Colombe Y, Steinmetz T, Dubois G, Linke F, Hunger D and Reichel J 2007 Strong atom-field coupling for Bose-Einstein condensates in an optical cavity on a chip *Nature* **450** 272
- [22] Raimond J M, Brune M and Haroche S 1997 Reversible decoherence of a mesoscopic superposition of field states *Phys. Rev. Lett.* **79** 1964
- [23] Mokarzel S G, Salgueiro A N and Nemes M C 2002 Modeling the reversible decoherence of mesoscopic superpositions in dissipative environments *Phys. Rev. A* **65** 044101
- [24] Wineland D and Dehmelt H 1975 Proposed  $10^{14} D\nu < \nu$  laser fluorescence spectroscopy on  $\text{Ti}^+$  mono-ion oscillator III (side band cooling) *Bull. Am. Phys. Soc.* **20** 637
- [25] Ollivier H and Zurek W H 2001 Quantum discord: A measure of the quantumness of correlations *Phys. Rev. Lett.* **88** 017901
- [26] Wootters W K 1998 Entanglement of formation of an arbitrary state of two qubits *Phys. Rev. Lett.* **80** 2245